Reduced elastic nonlinearity in Mn modified $0.6(Bi_{0.9}La_{0.1})FeO_3$–$0.4Pb(Ti,Mn)O_3$ high power piezoceramics

2012 Smart Mater. Struct. 21 065009

(http://iopscience.iop.org/0964-1726/21/6/065009)

IOP Publishing Smart Materials and Structures
Smart Mater. Struct. **21** (2012) 065009 (5pp) doi:10.1088/0964-1726/21/6/065009

Reduced elastic nonlinearity in Mn modified $0.6(Bi_{0.9}La_{0.1})FeO_3$–$0.4Pb(Ti, Mn)O_3$ high power piezoceramics

G Shi[1], L Feng[1], S Bu[1], W Ruan[2], G Li[2], T Yang[3] and J Cheng[1]

[1] School of Materials Science and Engineering, Shanghai University, Shanghai 200072, People's Republic of China
[2] Shanghai Institute of Ceramics, Chinese Academy of Science, Shanghai 200050, People's Republic of China
[3] Shanghai Synchrotron Radiation Facility, Shanghai Institute of Applied Physics, 201204, People's Republic of China

E-mail: jrcheng@staff.shu.edu.cn

Received 10 January 2012, in final form 28 March 2012
Published 18 May 2012
Online at stacks.iop.org/SMS/21/065009

Abstract
$0.6(Bi_{0.9}La_{0.1})FeO_3$–$0.4Pb(Ti_{1-x}Mn_x)O_3$ (BLF–PTM) piezoelectric ceramics with different Mn contents were fabricated by a sol–gel process combined with a solid-state reaction method. Coexistence of rhombohedral and tetragonal phases is detected in BLF–PTM. An asymmetric *P*–*E* loop with a large internal dipolar field of >20 kV cm^{-1} is observed in the poled BLF–PTM ceramics of $x = 0.01$ and 0.02, which is the typical characteristic of hard piezoelectric materials for higher power applications. The dielectric loss, planar coupling coefficient k_p, mechanical quality factor Q_m, vibration velocity, and Curie temperature of 0.006, 0.338, 418, 1.1 m s^{-1}, and 470 °C have been achieved for BLF–PTM with $x = 0.01$. Furthermore, the elastic nonlinear phenomena in BLF–PTM are investigated by measuring the vibration strain at high electric fields. Upon using Mn doping, BLF–PTM exhibits a large vibration strain and a small resonance frequency shift. The nonlinear elastic compliance of BLF–PTM for $x = 0.01$ and 0.02 was dramatically decreased by about two orders of magnitude compared to that of BLF–PT for $x = 0$.

1. Introduction

High power piezoelectric ceramic devices, such as ultrasonic motors, piezoelectric actuators and transformers, have been widely used in recent years [1–3]. Piezoelectric ceramics in these devices are often subjected to high electric fields or high stress with a large vibration velocity or displacement at resonance frequency. A shift of resonance frequency and current-jumping are usually observed under high applied fields, which significantly affects the stabilization of power devices [4, 5]. The field-dependent shift of resonance frequency results from the effect of elastic nonlinearity which is proportional to the nonlinear elastic compliance of materials. $Pb(Mg_{1/3}Nb_{2/3})O_3$–$PbTiO_3$ (PMNT), $Pb(Zn_{1/3}Nb_{2/3})O_3$–$PbTiO_3$ (PZNT) and hard $Pb(Zr, Ti)O_3$ (PZT) are the well investigated high power materials [6–9]. PMNT and PZNT have relatively larger nonlinear elastic compliance s_{11} of about 1.16×10^{-3} m^2 N^{-1} and 1.24×10^{-3} m^2 N^{-1} respectively, however, the hard PZT has a smaller s_{11} of 3.198×10^{-8} m^2 N^{-1} due to the restricted domain wall mobility [7, 9, 10].

$BiFeO_3$–$PbTiO_3$ (BF–PT) solid solutions, a kind of Pb reduced piezoelectric material, are potential alternatives for high power applications due to their high coercive and saturated fields, mechanical strengths and Curie temperature [11–14]. Lanthanum substitution has been reported to increase the piezoelectric properties of BF–PT significantly [11, 13]. The d_{33}, Pr and Ec of BF–PT with 10 at.% La can reach 186 pC N^{-1}, 26 μC m^{-2} and 28 kV cm^{-1}, respectively. The large coercive fields allow BF–PT to undergo high electric fields with high energy density. However, the high loss of >0.03 and the lower Q_m of

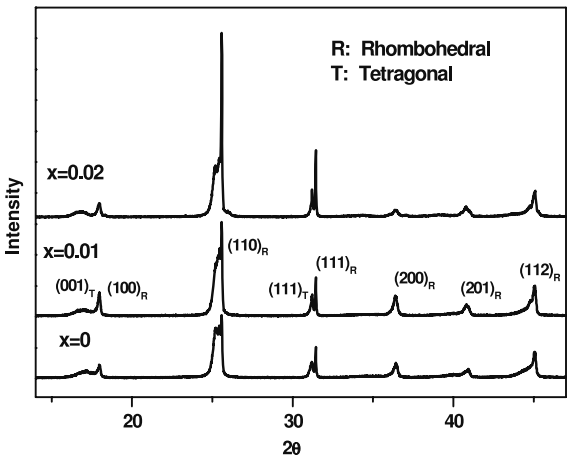

Figure 1. Shows HRXRD patterns of BLF–PTM for different Mn contents.

<100, become the major limit for BF–PT utilized in the high power devices. In this paper, Mn were introduced into $0.6(Bi_{0.9}La_{0.1})FeO_3$–$0.4PbTiO_3$ ceramics to decrease loss and enhance Q_m and k_p that influence the electromechanical properties of BF–PT under strong fields. The effects of Mn doping on the elastic nonlinearity of BLF–PTM ceramics were firstly investigated in terms of mechanical resonance frequency analysis. The nonlinear elastic compliance and electromechanical coefficients were calculated from the experimental data.

2. Experimental procedure

Ceramics of $0.6(Bi_{0.9}La_{0.1})FeO_3$–$0.4Pb(Ti_{1-x}Mn_x)O_3$ (BLF–PTM) for $x = 0$, 0.01, and 0.02 were fabricated by using the sol–gel derived BLF–PTM powders. Starting materials were bismuth nitrate, ferric nitrate, lead acetate, manganese acetate, and tetrabutyl titanate, which were of purities greater than 99%. The powders were calcined at 600 °C for 2 h and then pressed into pellets with diameter and thickness of about 12 and 1 mm respectively. The pellets were heated to 1070 °C, and then immediately cooled down to 800 °C for 4 h followed by a furnace cooling to room temperature.

High-resolution synchrotron x-ray diffraction (HRXRD) measurements were made at beam line BL14B1 of the Shanghai Synchrotron Radiation Facility at a wavelength of 1.2398 Å. Samples were disk type with diameter and thickness of about 10 and 0.25 mm respectively, and were electroded using a postfired silver paste. All samples were poled in a bath of silicon oil of 140 °C under DC field of 20–40 kV cm^{-1} for 20 min. The IEEE resonance and antiresonance method was utilized to calculate the electromechanical coupling factor. The piezoelectric constant was measured using the d_{33} meter (ZJ-3A). The *P–E* loops were measured by using a ferroelectric tester (premier II, Radiant Technologies Inc.). The vibration displacement was measured around resonance frequency under the planar coupling k_p model by a constant voltage method using a laser Doppler vibrometer (Polytec OFV-5000). A high speed bipolar amplifier (NF Electronic Instruments, model HSA 4011) in conjunction with an oscilloscope (Agilent 54622A) were utilized to apply an AC electrical excitation on specimens. The vibration strain was obtained from the vibration displacement divided by the radius of the specimen.

3. Results and discussion

Figure 1 shows HRXRD patterns of BLF–PTM for different Mn contents. BLF–PTM with different Mn contents has similar diffraction patterns. Analysis of XRD patterns reveals that all compositions possess a pure perovskite structure. The characteristic peaks of rhombohedral phase could be obviously detected in BLF–PTM, which is in accordance with traditional XRD patterns [15]. However, the additional peaks of $(001)_T$ and $(111)_T$ are also observed in HRXRD patterns of BLF–PTM. Rhombohedral and tetragonal phases actually coexist in BLF–PTM, which is the characterization of the morphotropic phase boundary.

Figures 2(a) and (b) show the polarization–electric field (*P–E*) loops of unpoled and poled BLF–PTM for different Mn contents. The area of hysteresis loop decreases significantly for specimens with Mn doping, indicating the great reduction of energy dissipation. Moreover, the *P–E* loops of poled BLF–PTM become more asymmetric with internal dipolar fields of 21.4 and 22.3 kV cm^{-1} for BLF–PTM of $x = 0.01$

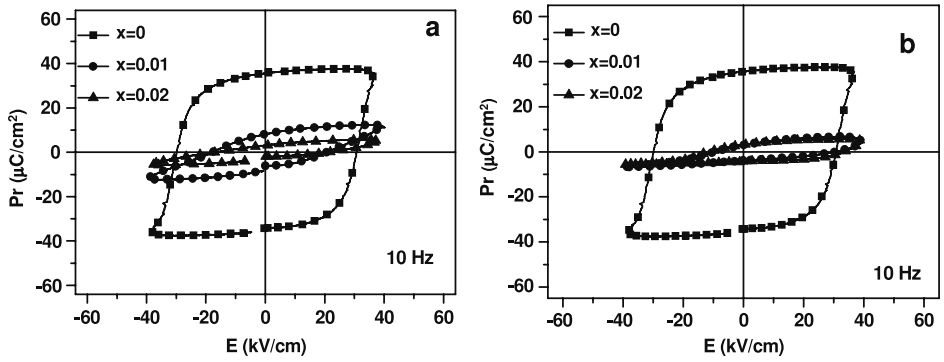

Figure 2. *P–E* loops of (a) unpoled and (b) poled BLF–PTM for $x = 0$, 0.01, and 0.02 taken at the maximum field of 40 kV cm^{-1}.

and 0.02 respectively, revealing a typical characteristic of hard piezoelectric materials [16]. When acceptor Mn^{2+} substitutes Ti^{4+} in the B-site, oxygen vacancies will be generated to keep the electrical neutrality. The domain wall could be pinned by oxygen vacancies which are easy to diffuse into domain boundaries [15]. The Mn^{2+}–oxygen vacancy defect dipolar exists in BLF–PTM and will be aligned under poling electric fields resulting in the large internal dipolar field [16, 17]. The domain wall motion and domain switching would be restrained by the internal dipolar field resulting in a reduction of electrical and mechanical dissipation.

The Curie temperature T_c of BLF–PTM is more than 450 °C, and slightly increases by Mn substitution. The $\tan\delta$ of Mn modified BLF–PTM is only 0.006, comparable to Pb-base high power ceramics, which is one fifth of BLF–PTM without Mn doping (table 1). The mechanical quality factors Q_m for BLF–PTM were obtained as 403 and 569 for $x = 0.01$ and 0.02, much larger than that of 96 for $x = 0$. In addition, Mn modified BLF–PTM samples show a high poling state [16], so BLF–PTM of $x = 0.01$ and 0.02 exhibits a higher piezoelectric constant d_{33} and planar electromechanical coupling coefficient k_p. Mn modified BLF–PTM could be an excellent high power ceramic with larger vibration velocity which is proportional to the product of the mechanical quality factor and electromechanical coupling coefficient. The maximum vibration velocities of 1.1 m s^{-1} and 0.8 m s^{-1} have been achieved at the resonance frequency for BLF–PTM of $x = 0.01$ and 0.02 respectively, which are about 3.7 and 2.7 times larger than that of commercialized hard PZT (0.3 m s^{-1}) piezoelectric ceramics.

Figure 3 shows the vibration strain of BLF–PTM for $x = 0$, 0.01, and 0.02 as a function of frequency at different applied fields. The strain–frequency (ε–f) curves exhibit a resonance peak typical of that of a linear harmonic oscillator. Meanwhile, the resonance frequency of BLF–PTM shifts to lower frequency with increasing applied fields, which is an evident elastic nonlinearity of piezoelectric materials [7, 9]. The resonance peak of BLF–PTM for $x = 0.01$ and 0.02 looks more asymmetric at higher applied field. Furthermore, the widths of resonance peaks for BLF–PTM of $x = 0.01$ and 0.02 are narrower than that for BLF–PTM of $x = 0$, implying that a higher mechanical quality factor Q_m has been achieved for BLF–PTM with Mn addition at a higher applied field [7]. In addition, it can be seen that the specimen with Mn doping could be driven at a relatively small electric field, however, giving a larger vibration strain and thus a larger vibration velocity.

It is noticed that the effective resonance frequency, f_r(eff), and strain, ε, of BLF–PTM are strongly dependent on the applied fields. The correlation between f_r(eff) and ε can be written by the following empirical formula [18, 19], in which the contribution of elastic nonlinearity to f_r(eff) was considered.

$$f_r(\text{eff}) = f_r^{\text{lin}} - \Delta f_r^{\text{nonlin}}\varepsilon^2 = f_r^{\text{lin}} + \frac{3\alpha}{8f_r^{\text{lin}}}\varepsilon^2 \qquad (1)$$

where f_r^{lin} is the linear resonance frequency, $\Delta f_r^{\text{nonlin}}$ is a parameter which is relative to the resonance frequency shift, and α is the third-order nonlinear elastic constant. The equation (1) suggested that the shift in resonance frequency under high electric fields is due to the third-order nonlinear elastic effect [18].

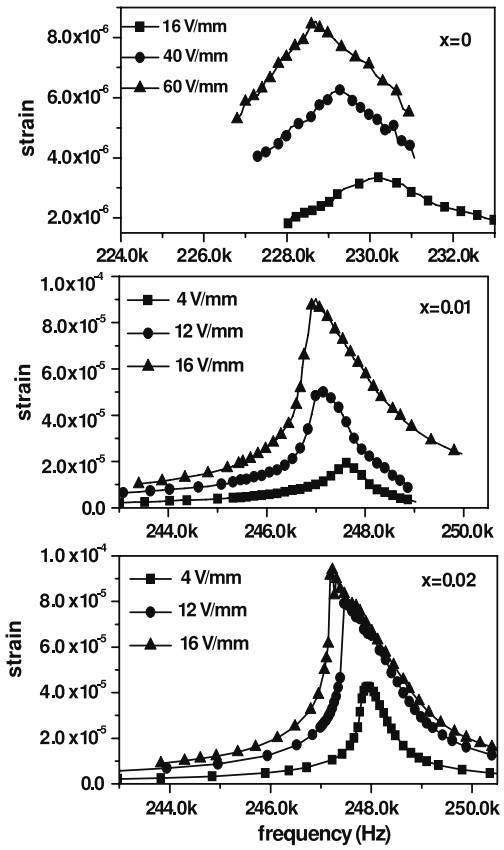

Figure 3. Vibration strain of BLF–PTM for $x = 0$, 0.01, and 0.02 as a function of frequency at different applied fields.

Figure 5 plots the curve of measured f_r(eff) versus ε^2 for BLF–PTM of $x = 0$, 0.01, and 0.02. It can be seen that f_r(eff) decreases obviously when the higher ε is achieved, exhibiting a linear relationship with ε^2. To achieve a certain magnitude of ε, BLF–PTM with Mn doping must be driven by the field with relatively higher frequency. The effective elastic compliance s_p(eff) of BLF–PTM is a function of the reverse of f_r^2(eff), as shown in equation (2).

$$s_p(\text{eff}) = \frac{1}{4D^2 f_r^2(\text{eff})\rho} \qquad (2)$$

where D and ρ are the diameter and density of the sample respectively. Similarly to f_r(eff), the s_p(eff) under electric fields consists of both linear and nonlinear parts being proportional to ε^2, which is described by

$$s_p(\text{eff}) = s_p^{\text{lin}} + s_{pp}^{\text{nonlin}}\varepsilon^2 \qquad (3)$$

where s_p^{lin} is the linear (fundamental) elastic compliance, s_{pp}^{nonlin} is the third-order nonlinear elastic compliance. The linear relationship between s_p(eff) and ε^2 for BLF–PTM is evidenced in figure 4. It is found that the s_p(eff) slightly increases with the increase of ε^2. The s_p(eff) of BLF–PTM

Table 1. Piezoelectric and electromechanical properties of BLF–PTM.

x	ε (1 kHz)	$\tan\delta$ (1 kHz)	d_{33} (pC N^{-1})	k_p	Q_m	V_0 (m s^{-1})	T_c (°C)
0	649	0.033	103	0.21	96	0.14	455
0.01	380	0.006	124	0.34	403	1.1	470
0.02	350	0.006	107	0.33	569	0.83	495

Table 2. Linear and nonlinear parameters of BLF–PTM for $x = 0$, 0.01, and 0.02.

x	f_r^{lin} (Hz)	Δf_r^{nonlin} (Hz)	s_p^{lin} ($\times 10^{-11}$ m^2 N^{-1})	s_{pp}^{nonlin} (m^2 N^{-1})	k_p^{lin}	k_{pp}^{nonlin}
0	230 635	7.7156×10^{12}	0.6538	4.0561×10^{-4}	0.2122	1.619×10^{9}
0.01	247 660	3.1438×10^{10}	0.5221	1.3503×10^{-6}	0.353	5.524×10^{5}
0.02	248 144	2.7655×10^{10}	0.5451	1.2236×10^{-6}	0.3462	3.608×10^{5}

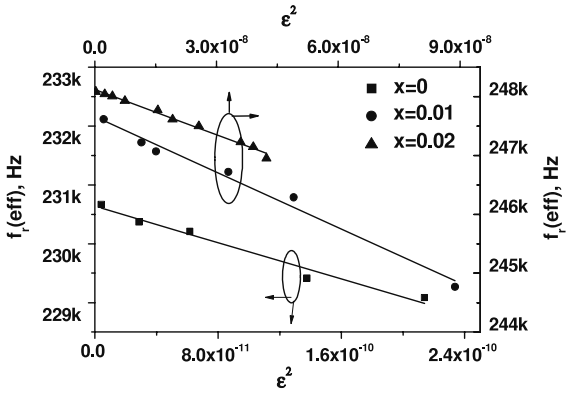

Figure 4. Effective resonance frequency of BLF–PTM for $x = 0$, 0.01, and 0.02 as a function of ε^2.

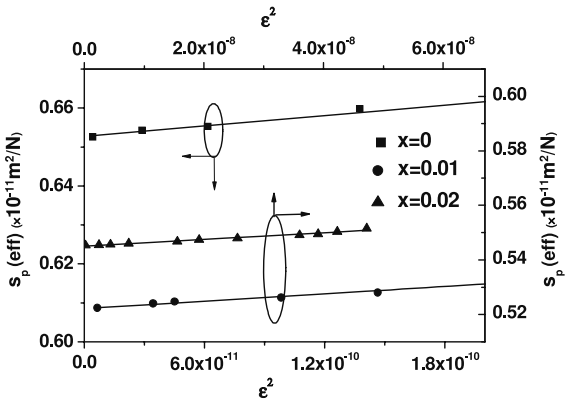

Figure 5. Effective elastic compliance of BLF–PTM for $x = 0$, 0.01, and 0.02 as a function of ε^2.

for $x = 0.01$ and 0.02 is lower than that of BLF–PT without Mn addition. The lowest s_p(eff) of about 0.61×10^{-11} N m^{-2} is observed for BLF–PTM of $x = 0.01$.

According to equations (1) and (3), the linear and nonlinear contribution to the f_r(eff) and s_p(eff) could be distinguished by linearly fitting the measured data shown in figures 3 and 4. The calculated f_r^{lin} and Δf_r^{nonlin}, s_p^{lin} and s_{pp}^{nonlin} of BLF–PTM of different Mn contents are listed in table 2. The linear and nonlinear electromechanical coupling coefficients are also analyzed and given in table 2. The linear and nonlinear electromechanical coupling coefficients follow the relation:

$$k_p(\text{eff}) = k_p^{lin} + k_{pp}^{nonlin}\varepsilon^2 \tag{4}$$

where k_p^{lin} is the linear (fundamental) electromechanical coupling coefficient, k_{pp}^{nonlin} is the nonlinear electromechanical coupling coefficient and is related to the third-order nonlinear elastic compliance.

It is found that f_r^{lin} of BLF–PTM increases with addition of Mn contents, being in agreement with the reduction of s_p^{lin}. Upon using the Mn dopants, the Δf_r^{nonlin} and s_{pp}^{nonlin} decrease about two orders of magnitude with respect to those of BLF–PTM for $x = 0$, demonstrating the great reduction of the nonlinear contribution to f_r(eff) and s_p(eff) of BLF–PTM under the applied fields. Moreover, the nonlinear electromechanical coupling coefficient of BLF–PTM for $x = 0.01$ and 0.02 is about four orders of magnitude lower than that for $x = 0$.

It has been known that the nonlinear elastic effect is related to the motion of domains, which could induce a shift of resonance frequency [19]. Upon using Mn substitutions, oxygen vacancies are generated and form pinning effects in domain walls, decreasing the mobility of domain wall. In addition, a large internal dipolar field is produced in BLF–PTM due to the orientation of dipolar defects. The dipolar fields would remain stable in the process of mechanical domain rearrangement, and facilitate the recovery of the original domain configuration [10]. Thus, the motion of the ferroelectric–ferroelastic domain (non-180° domain) wall, the origin of the elastic nonlinearity [12, 20–23], could be effectively restrained by the internal field in BLF–PTM. The smaller nonlinear elastic compliance of BLF–PTM for $x = 0.01$ and 0.02 is in agreement with the smaller shift of resonance frequency of these specimens. The nonlinear elastic effect consequently results in the nonlinearity of electromechanical coupling coefficient under high applied fields. The smaller electromechanical nonlinearities of BLF–PTM for $x = 0.01$ and 0.02 are attributed to the stabilized domain configuration.

4. Conclusions

BLF–PTM exhibits an enhanced electromechanical quality factor Q_m, planar coupling coefficient k_p and large vibration velocity. Under higher applied fields, the nonlinear elastic effects are observed in BLF–PTM. However, the nonlinear contribution to the piezoelectric resonance frequency, electromechanical coupling coefficient, and the elastic compliance has been effectively restrained by introducing Mn dopants in BLF–PTM. The domain wall pinning effects and large internal dipolar field in BLF–PTM of $x = 0.01$ and 0.02 contribute to the decrease in the mobility of ferroelectric–ferroelastic domains resulting in the great reduction of the elastic compliance and a smaller shift of resonance frequency.

Acknowledgments

This work was supported by the Shanghai education development foundation under grant no. 08SG41, National Nature Science Foundation of China under grant no. 50872080, and the Innovational Foundation of Shanghai University.

References

[1] Uchino K 1998 *Smart Mater. Struct.* **7** 273
[2] Shin H, Ahn H and Han D Y 2005 *Mater. Chem. Phys.* **92** 616
[3] Kanda T, Makino A, Ono T, Suzumori K, Morita T and Kurosawa M K 2006 *Sensors Actuators* A **127** 131
[4] Seyit O, Tuncdemir S, Zhuang Y and Uchino K 2009 *Japan. J. Appl. Phys.* **48** 056509
[5] Tashiro S, Ishii L and Nagata L 2003 *Japan. J. Appl. Phys.* **42** 6068
[6] Hagiwata M, Hoshina T, Takeda H and Tsurumi T 2010 *Japan. J. Appl. Phys.* **49** 09MD04
[7] Priya S, Viehland D, Carazo A V, Ryu J and Uchino K 2001 *J. Appl. Phys.* **90** 1469
[8] Chen Y, Hirose S, Viehland D, Takahashi S and Uchino K 2000 *Japan. J. Appl. Phys.* **39** 4843
[9] Priya S, Viehland D, Ryu J, Uchino K, Yamasjota Y and Luo H 2001 *Japan. J. Appl. Phys.* **40** 6487
[10] Hall D A 2001 *J. Mater. Sci.* **36** 4575
[11] Cheng J, Meng Z and Cross L E 2005 *J. Appl. Phys.* **98** 084102
[12] Kounga Njiwa A B, Aulbach E, Rödel J, Turner S L, Comya T P and Bell A J 2006 *J. Am. Ceram. Soc.* **89** 1761
[13] Leist T, Webber K G, Jo W, Aulbach E, Rödel J, Prewitt A D, Jones J L, Schmidlin J and Hubbard C R 2010 *Acta Mater.* **58** 5962
[14] Leist T, Webber K G, Jo W, Aulbach E, Jones J L and Rödel J 2011 *J. Appl. Phys.* **109** 054109
[15] Shi G, Chen J, Zhou L, Yu S, Cheng J, Hong L and Li G 2011 *Curr. Appl. Phys.* doi:10.1016/j.cap.2011.03.019
[16] Tan Q, Li J F and Viehland D 1997 *Phil. Magn.* B **76:1** 59
[17] Gao Y, Uchino K and Vielhland D 2007 *J. Appl. Phys.* **101** 1
[18] Johnson P A, Zinszner B and Rasolofosaon P J 1996 *J. Geophys. Res.* **101** 11553
[19] Chen Y H and Uchino K 2001 *J. Appl. Phys.* **89** 3928
[20] Damjanovic D and Demartin M 1996 *Appl. Phys. Lett.* **68** 3046
[21] Takahashi S, Yamamoto M and Sasaki Y 1998 *Japan. J. Appl. Phys.* **37** 5292
[22] Tashiro S, Murata T, Ishii K and Igarashi H 2001 *Japan. J. Appl. Phys.* **40** 5679
[23] Wang Q, Zhang Q, Xu B, Liu R and Cross L E 1999 *J. Appl. Phys.* **86** 3352